Scientia Iranica D (2014) 21(6), 2186–2199

SCIENTIA IRANICA

Sharif University of Technology

Scientia Iranica

Transactions D: Computer Science & Engineering and Electrical Engineering

www.scientiairanica.com

Spatial diversity gain of MIMO single frequency network in passive coherent location

M. Radmard*, M. Nazari Majd, M.M. Chitgarha, B.H. Khalaj and M.M. Nayebi

School of Electrical Engineering, Sharif University of Technology, Tehran, Iran.

Received 24 December 2012; received in revised form 23 October 2013; accepted 8 April 2014

KEYWORDS

Multi-input multi-output;
Spatial diversity;
Single frequency network;
Passive coherent location.

Abstract. Recently, it has been shown that applying MIMO technology, i.e. using multiple antennas at the transmit side and multiple antennas at the receive side, improves the performance of object detection and localization. In such scenarios, the spatial diversity specifically helps overcome the fading of the cross section of the object, leading to reduced probability of missed detection. Such a phenomenon is, in fact, the dual of probability of bit error reduction in communication systems due to diversity gain. Despite the importance of such performance enhancement, this subject has not been sufficiently investigated in the PCL (Passive Coherent Location) schemes, where the transmitters (or illuminators of opportunity) used for localization are already present in the environment. Especially, in cases where the transmitters are working in a SFN (Single Frequency Network), such as the DVB-T (Digital Video Broadcasting-Terrestrial) signal, and all are transmitting the same signal, the situation becomes of higher importance. Obviously, the effect of the SFN environment invalidates the assumption of sending orthogonal waveforms traditionally used in localization schemes. In this paper, we design the Neyman-Pearson detector for a PCL scheme and show that we can achieve the desired diversity gain for such a design as well.

1. Introduction

1.1. Passive coherent location

PCL has attracted much attention due to its advantages over active detection schemes. Low-cost passive localization, which requires no frequency allocation, is a good solution for increased localization at a lower cost [1]. The feasibility of different kinds of opportunistic signal used for this application has been investigated earlier, for example, in the case of FM [2], analogue TV [3,4], DTV (Digital TV) [5-7], satellite systems [8], and GSM [9,10]. New digital signals, such as Digital Audio/Video Broadcast (DAB/DVB), are also excellent candidates [11-13], as they are widely available and can be easily decoded.

In traditional active systems, the object's range is defined by comparing the time of the transmitted and received pulses. However, such information is not directly available in the case of the PCL. Instead, two antennas are used: one for receiving the signal directly from its main source without reflections from objects of interest (reference antenna) and the other for collecting the reflections from objects in the environment (reflection antenna). Figure 1 depicts the overall structure of the PCL.

Detection is done through computation of CAF (Cross Ambiguity Function) computed according to Eq. (1). It is a criterion of how much correlation exists between the reference and the reflection signal. A given CAF's peak in a range-Doppler cell is a representative

*. *Corresponding author. Tel.: +98 21 66163667*
E-mail addresses: radmard@ee.sharif.ir (M. Radmard); nazarimajd@ee.sharif.ir (M. Nazari Majd); chitgarha@ee.sharif.ir (M.M. Chitgarha); khalaj@sharif.ir (B.H. Khalaj); nayebi@sharif.ir (M.M. Nayebi)

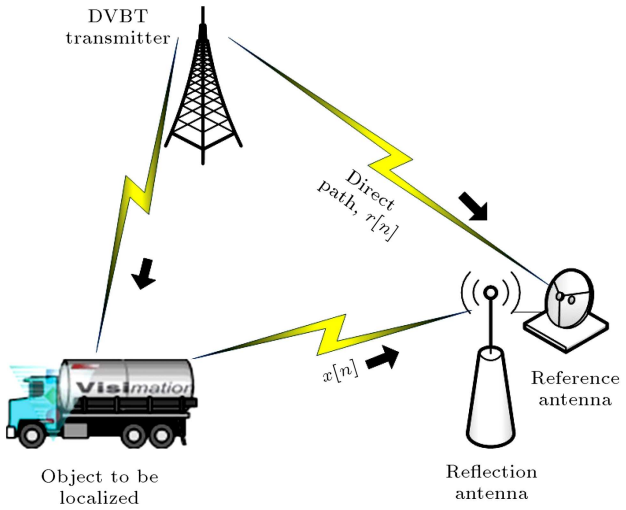

Figure 1. Structure of a passive scheme.

of a target in that range and Doppler frequency.

$$|\chi(\tau,\nu)|^2 = |\frac{1}{N}\sum_{n=1}^{N} x(n)r^*(n-\tau)e^{-j\frac{2\pi}{N}\nu n}|^2, \qquad (1)$$

where $x[n]$ is the signal at the target channel, $r[n]$ is the reference signal, ν is the Doppler shift, τ is the sample shift and N is the number of samples collected.

1.2. Multi-Input Multi-Output (MIMO), an upcoming technology for localization

Recently, use of MIMO techniques for improving the performance of localization schemes has attracted much attention. Generally, such MIMO schemes are divided into two categories: widely separated [14] and colocated antennas [15]. In the former case, multiple transmitters and receivers that are widely separated are used. The main advantage of such configuration is that by obtaining signals from different angles, the probability of missed detection decreases; a concept also known as spatial diversity in MIMO communication. In fact, as shown in [14] the concepts of spatial diversity and multiplexing gain emerge in a manner dual to the ideas in traditional MIMO communication. On the other hand, in the case of colocated antennas, transmitters and receivers are located at nearby positions. Such configuration is similar to phased array systems, with the difference that signals emitted by each antenna can be totally uncorrelated with the other antennas. Recent studies have shown that the widely separated antenna configuration leads to enhanced detection performance (Diversity Gain) [16-18], better tracking [19], and higher resolution (spatial multiplexing gain) [20]. On the other hand, improved parameter identifiability [21], better target identification and classification [22], direct applicability of adaptive arrays for detection and parameter estimation [23,24], and enhanced flexibility for transmit beam-pattern design [25,26] are achieved by the colocated antennas configuration.

1.3. MIMO passive coherent location, a new concept

By combining the ideas of passive and MIMO localization, one can achieve the benefits of both schemes by using multiple receivers to detect objects illuminated by multiple noncooperative transmitters. In general, the transmitters may be sending different signals (e.g. a broadcasting FM radio with a GSM base station). One case of high interest is the DVB-T SFN (Single Frequency Network), in which all TV transmitters are broadcasting the same data at the same frequency band.

1.4. Diversity gain in MIMO PCL

Multipath fading is one of the most fundamental features of wireless channels. Because multiple received replicas of the transmitted signal sometimes combine destructively, there is a significant probability of severe fading. Without proper means to mitigate such fading scenarios, ensuring reasonable reliability requires large power margins [27]. One of the most powerful techniques to mitigate the effects of fading is to use the diversity combining of independently fading signal paths. Diversity-combining uses the fact that independent signal paths have a low probability of experiencing deep fades simultaneously. Thus, the idea behind diversity is to send the same data over independent fading paths. These independent paths are combined in such way that the fading effect on the resulting signal is reduced. There are many ways of achieving independent fading paths in a wireless system. One method is to use multiple transmit or receive antennas in an antenna array configuration, where array elements are separated enough in space [28]. Therefore, rather than making the success of a transmission entirely dependent on a single fading realization, the probability of failure is reduced by exploiting multiple such realizations [27], leading to spatial diversity.

Mathematically, in MIMO communication, diversity gain is defined at high SNR values as [29]:

$$\lim_{\mathrm{SNR}\to\infty} \frac{\log P_e}{\log \mathrm{SNR}} = -d, \qquad (2)$$

where P_e is the error probability and d denotes diversity gain. It should be noted that in MIMO detection, P_e is replaced by P_{miss} (missed detection probability).

It is well known that if the object to be localized is much greater than the wavelength of a transmitted signal, the received signal will be random and fluctuating in time. Signal fluctuations deteriorate detection performance [30], as the object's cross section parallels the role of the random wireless channel. The reason is that if an object's size is much greater than the wavelength of a transmitting signal, the difference in distances from scatterers to receiver antennas significantly exceeds the wavelength. Consequently, the

phase of signals arriving from different scatterers may fluctuate significantly. Even small random rotations of a real object about its center of mass lead to significant changes in distance, and hence, sharp phase variations of signals received from different scatterers [30]. Correspondingly, parallel to MIMO communication, it is possible to obtain diversity by looking at an object from different angles.

Obtaining diversity gain in MIMO detection has recently been highly investigated, [17,31,32]. But, such analysis has not yet been performed in the case of applying MIMO to PCL. The main difference is that here, we use noncooperative transmitters whose transmitted signal is not under control. Especially in a DVB-T network of transmitters, all the transmitters send the same signal in the same frequency.

In previous works on MIMO detection, it is assumed to have active transmit antennas. Mostly, it is assumed that the transmitted waveforms are orthogonal [33-38], so that they can be separated at the receiver side, a property that is not true in the case of MIMO PCL (especially DVB-T, which is almost the focus of PCL because of its unique properties for radar application and also being broadcasted in a network, making it quite suitable for MIMO application). For example, in [31], it is assumed that:

$$\int_{-\infty}^{\infty} s_k(t)s_{k'}^*(t)dt \approx \begin{cases} 1 & \text{if } k = k' \\ 0 & \text{if } k \neq k' \end{cases} \quad (3)$$

Also, in [32], the authors want to obtain the diversity gain when the waveforms are not orthogonal (but not fully correlated). They use an orthogonal basis to show the non-orthogonal transmitted waveforms, where the dimension of this basis is M_n, which is less or equal to the number of transmitters (being equal in the case of transmitting orthogonal signals). Finally, they have concluded that:

$$d = \min\{NM_n, Q\},$$

where Q is the number of scatterers. However, in our case (MIMO SFN PCL e.g. DVB-T), $M_n = 1$ (all of the transmitters are sending the same signal) and, therefore, the diversity gain is not proportional to the number of transmitters, according to the results of the aforementioned paper.

In addition, in [39], the optimal test statistics for a statistical MIMO radar (or equivlently a MIMO radar with widely separated antennas) using non-orthogonal signals are derived. However, the authors in [39] have not considered the fact that different paths experience different loss paths from the transmitter to the target to the receiver. Indeed, in a MIMO radar with widely separated antennas, the transmitted signals arrive at the receiver with different delays and different path losses, which is ignored in the signal model of [39].

In this paper, we want to see if we can obtain the main advantage of the MIMO technique (i.e. diversity gain) in MIMO DVB-T based passive radar (PCL). In Section 2, we will design the detector structure for a MIMO PCL in a single frequency network. P_{miss} will be derived in a closed form, and obtaining a spatial diversity gain proportional to the product of the number of the transmit and receive antennas will be proved. Simulations for different environments are included in Section 3. Finally, Section 4 concludes the paper.

2. Detection in the MIMO SFN PCL

Assume that there are M illuminators of opportunity (e.g. broadcasting DVB-T signals in a Single Frequency Network), N receive sensors and an object to be localized. For simplification, we have assumed that the object to be localized has no Doppler, although such an assumption is not critical in our derivations. The reflection antenna is assumed to be omnidirectional, collecting signals arriving from all directions. An important obstacle in passive coherent location is the Direct Path Interference (DPI), which should be rejected from the reflection channel. Different schemes to overcome such an effect have been recently presented for PCL systems, where satisfying practical results have been achieved [2,7,40]. Therefore, in this paper, we assume that such schemes have been incorporated and the remaining DPI effect is negligible.

At the receiver side, after DPI cancellation, the signal is passed through a CAF processor to obtain the delays and Doppler frequencies of different echoes collected from the object to be localized. The threshold at the output of the CAF processor for declaring that an object is detected is determined by the desired false alarm rate (P_{fa}). In the case of MIMO PCL, the signal received at the n'th receive antenna is presented by Eq. (4):

$$r_n(t) = \sqrt{\frac{E_t}{L}} \sum_{i=1}^{M} \frac{\alpha_i^n}{r_{1i}r_{2i}} s(t - \tau_i) + n(t), \quad (4)$$

where $s(t)$ is the transmitted signal (the same for all transmitters), r_{1i} and r_{2i} are the distance from the transmitter to the target and the distance from the target to the receiver, respectively, M is the number of transmitters, α_i is the cross-section gain of the object illuminated by the signal transmitted from the ith transmitter, E_t is the energy of the transmitted signal, L is the channel loss, and τ_i denotes its delay.

We define the probability of missed detection (P_{miss}) as the probability that we miss all echoes of the desired object (similar to [41]).

$$P_{\text{miss}} = \prod_{m=1}^{M} \prod_{n=1}^{N} P_{\text{miss}}^{mn}, \tag{5}$$

where P_{miss}^{mn} is the probability of missing the object's echo from the m'th transmitter at the n'th receiver.

The reason for considering the case of missing all echoes of the object as missed detection is that we can design the detector such that after detecting one or two echoes, the threshold can be reduced adaptively in order to detect a sufficient number of echoes (e.g. in the case of one receiver three echoes). Although, by such an approach P_{fa} would increase, the data association algorithm we have developed in [42], used to associate these echoes to objects, will eliminate such false echoes. In fact, the target localization schemes developed for MIMO DVB-T based PCL, such as [42], assume that each object's echo is detected with a given probability of detection. So, even if some (but not all) echoes are missed, it might still be possible to localize the object using the remaining echoes' TDoAs (Time Difference of Arrival). Such algorithms would definitely fail if no echo from the object is detected at the receiver. However, as the number of detected echoes decreases, the probability of correct localization decreases as well. Another reason is that we can localize the object by other techniques, such as Direction-Of-Arrival (DOA) estimation, after detecting it at an acceptable P_{miss} level. In addition, the reason for multiplying the missed detection probabilities comes from the fact that the antennas are widely separated, resulting in decorrelated echoes [14].

2.1. Problem formulation

Next, we explore the probability of missed detection in the MIMO PCL. The existence of a target in a specific bistatic range cell is a random process with unknown probability. We use a Neyman-Pearson detector because a priori probabilities are unknown. Consequently, we compare the likelihood ratio, $L(\mathbf{y})$, with threshold η to derive the false alarm probability. So, at the n'th receiver, for a specific bistatic range cell, we have:

$$\mathcal{H}_0 : \mathbf{y} = \mathbf{n},$$

$$\mathcal{H}_1 : \mathbf{y} = \mathbf{n} + l\mathbf{s}, \tag{6}$$

where $\mathbf{y}$, $\mathbf{s}$ and $\mathbf{n}$ are discrete samples of signals, $r_n(t)$, $s(t-\tau_m)$ and $n(t)$, with length N_T, respectively. Consequently, $\mathbf{y}$ is the received signal vector at the n'th receiver and $\mathbf{s}$ is the signal from the m'th transmitter.

In general, the signal is complex, i.e. $\mathbf{s} = \mathbf{s}'e^{j\phi}$, where $\mathbf{s}' = |\mathbf{s}|$ is real. Multiplying $e^{-j\phi}$ by both sides of Eq. (6), we have:

$$\mathcal{H}_0 : e^{-j\phi}\mathbf{y} = \mathbf{y}' = e^{-j\phi}\mathbf{n} = \mathbf{n}',$$

$$\mathcal{H}_1 : e^{-j\phi}\mathbf{y} = \mathbf{y}' = e^{-j\phi}\mathbf{n} + l\mathbf{s}' = \mathbf{n}' + l\mathbf{s}', \tag{7}$$

where $\mathbf{n}'$ denotes complex noise with the same properties of $\mathbf{n}$. As $l\mathbf{s}'$ is real, only the real part of noise is important. As a result, the hypothesis test is simplified as below:

$$\mathcal{H}_0 : \mathbf{y} = \mathbf{n}, \quad \mathcal{H}_1 : \mathbf{y} = \mathbf{n} + l\mathbf{s}, \tag{8}$$

where, for simplification, we have denoted $\text{Re}(\mathbf{y}')$ by $\mathbf{y}$, $\mathbf{s}'$ by $\mathbf{s}$, and $\text{Re}(\mathbf{n}')$ by $\mathbf{n}$. Therefore, in the rest of the equations, the signals are real.

It should be noted that the signals presented in other bistatic range cells that make interference in this range cell, are included in $\mathbf{n}$. For example, for the DVB-T signal, which is the case of interest, due to its highly randomized nature, it can be considered as white noise [6,43]. Consequently, the signals of other cells constitute a white noise component for $\mathbf{n}$. Here, we assume the general case of $\mathbf{n} \sim \mathcal{N}(0, \mathbf{R})$. In subsequent sections, we will consider four different cases for $\mathbf{R}$ to represent different situations of considering noise and clutter.

For $\mathcal{H}_1$, where we assume the target is present, we assume its RCS follows the Swerling I model (also called *Rayleigh scatter*). If σ^2 represents RCS, the distribution function of σ is:

$$f_\sigma(\sigma) = \frac{\sigma}{\sigma_0^2} e^{-\frac{\sigma^2}{2\sigma_0^2}}, \tag{9}$$

where σ_0^2 is the RCS average value.

In Eq. (8), the coefficient l (the gain experienced by the signal from the transmitter to the receiver) is:

$$l = \frac{\sigma v}{r_{1i} r_{2i}}, \tag{10}$$

where:

$$v = \sqrt{\frac{P_t G_t G_r I_p \lambda^2}{(4\pi)^3 L_c L_r}}. \tag{11}$$

In the above equation, P_t is the transmitted power, G_t and G_r are the transmitting and receiving antenna gains, respectively, I_p is the processing gain at the receiver, L_c is the scattering loss, and L_r is the receiver loss. Therefore, the distribution function of l is:

$$f_L(l) = \frac{\sigma}{\sigma_t^2} e^{-\frac{\sigma^2}{2\sigma_t^2}}, \tag{12}$$

where:

$$\sigma_t^2 = \frac{P_t G_t G_r I_p \sigma_0^2 \lambda^2}{(4\pi)^3 r_{1i}^2 r_{2i}^2 L_c L_r}. \tag{13}$$

Now, considering the above equations:

$$f_{\mathbf{Y}}(\mathbf{y}|\mathcal{H}_0) = f_{\mathbf{n}}(\mathbf{y}) = \frac{1}{(2\pi)^{\frac{N_T}{2}}|\mathbf{R}|^{\frac{1}{2}}} e^{-\frac{\mathbf{y}^T\mathbf{R}^{-1}\mathbf{y}}{2}}, \quad (14)$$

$$f_{\mathbf{Y}}(\mathbf{y}|\mathcal{H}_1, l) = f_{\mathbf{n}}(\mathbf{y} - l\mathbf{s}) = \frac{1}{(2\pi)^{\frac{N_T}{2}}|\mathbf{R}|^{\frac{1}{2}}} e^{-\frac{(\mathbf{y}-l\mathbf{s})^T\mathbf{R}^{-1}(\mathbf{y}-l\mathbf{s})}{2}}, \quad (15)$$

$$\begin{aligned} f_{\mathbf{Y}}(\mathbf{y}|\mathcal{H}_1) &= \int_0^\infty f_{\mathbf{Y}}(\mathbf{y}|\mathcal{H}_1, l) f_L(l) dl \\ &= \int_0^\infty \frac{1}{(2\pi)^{\frac{N_T}{2}}|\mathbf{R}|^{\frac{1}{2}}} e^{-\frac{(\mathbf{y}-l\mathbf{s})^T\mathbf{R}^{-1}(\mathbf{y}-l\mathbf{s})}{2}} \frac{l}{\sigma_t^2} e^{-\frac{l^2}{2\sigma_t^2}} dl \\ &= \frac{e^{-\frac{1}{2}\mathbf{y}^T\mathbf{R}^{-1}\mathbf{y}}}{(2\pi)^{\frac{N_T}{2}}|\mathbf{R}|^{\frac{1}{2}}\sigma_t^2} \\ &\times \int_0^\infty e^{-\frac{1}{2}l^2\mathbf{s}^T\mathbf{R}^{-1}\mathbf{s} + \frac{1}{2}l(\mathbf{s}^T\mathbf{R}^{-1}\mathbf{y} + \mathbf{y}^T\mathbf{R}^{-1}\mathbf{s}) - \frac{l^2}{2\sigma_t^2}} l dl \\ &= \frac{e^{-\frac{1}{2}\mathbf{y}^T\mathbf{R}^{-1}\mathbf{y}}}{(2\pi)^{\frac{N_T}{2}}|\mathbf{R}|^{\frac{1}{2}}\sigma_t^2} \\ &\times \int_0^\infty e^{-\frac{1}{2}l^2(\mathbf{s}^T\mathbf{R}^{-1}\mathbf{s} + \frac{1}{\sigma_t^2}) + \frac{1}{2}l(\mathbf{s}^T\mathbf{R}^{-1}\mathbf{y} + \mathbf{y}^T\mathbf{R}^{-1}\mathbf{s})} l dl \\ &= \frac{e^{-\frac{1}{2}\mathbf{y}^T\mathbf{R}^{-1}\mathbf{y}}}{(2\pi)^{\frac{N_T}{2}}|\mathbf{R}|^{\frac{1}{2}}\sigma_t^2} \int_0^\infty e^{-C_1^2 l^2 + C_2 l} l dl, \end{aligned} \quad (16)$$

where:

$$C_1^2 = \frac{1}{2}(\mathbf{s}^T\mathbf{R}^{-1}\mathbf{s} + \frac{1}{\sigma_t^2}), \quad (17)$$

$$C_2 = \frac{1}{2}(\mathbf{s}^T\mathbf{R}^{-1}\mathbf{y} + \mathbf{y}^T\mathbf{R}^{-1}\mathbf{s}), \quad (18)$$

so:

$$\begin{aligned} f_{\mathbf{Y}}(\mathbf{y}|\mathcal{H}_1) &= \frac{e^{-\frac{1}{2}\mathbf{y}^T\mathbf{R}^{-1}\mathbf{y}}}{(2\pi)^{\frac{N_T}{2}}|\mathbf{R}|^{\frac{1}{2}}\sigma_t^2} \int_0^\infty l e^{-(C_1 l - \frac{C_2}{2C_1})^2 + \frac{C_2^2}{4C_1^2}} dl \\ &= \frac{e^{-\frac{1}{2}\mathbf{y}^T\mathbf{R}^{-1}\mathbf{y} + \frac{C_2^2}{4C_1^2}}}{(2\pi)^{\frac{N_T}{2}}|\mathbf{R}|^{\frac{1}{2}}\sigma_t^2} \int_0^\infty l e^{-(C_1 l - \frac{C_2}{2C_1})^2} dl \\ &= \frac{e^{-\frac{1}{2}\mathbf{y}^T\mathbf{R}^{-1}\mathbf{y} + \frac{C_2^2}{4C_1^2}}}{(2\pi)^{\frac{N_T}{2}}|\mathbf{R}|^{\frac{1}{2}}\sigma_t^2 C_1^2} \\ &\times \left(\int_{-\frac{C_2}{2C_1}}^\infty x e^{-x^2} dx + \int_{-\frac{C_2}{2C_1}}^\infty \frac{C_2}{2C_1} e^{-x^2} dx \right) \\ &= \frac{e^{-\frac{1}{2}\mathbf{y}^T\mathbf{R}^{-1}\mathbf{y} + \frac{C_2^2}{4C_1^2}}}{(2\pi)^{\frac{N_T}{2}}|\mathbf{R}|^{\frac{1}{2}}\sigma_t^2 C_1^2} \\ &\times \left(-\frac{1}{2} e^{-x^2} |_{-\frac{C_2}{2C_1}}^\infty + \frac{\sqrt{2\pi} C_2}{2\sqrt{2} C_1} Q\left(-\frac{\sqrt{2} C_2}{2C_1} \right) \right), \end{aligned} \quad (19)$$

where:

$$Q(x) = \int_x^\infty \frac{1}{\sqrt{2\pi}} e^{-\frac{u^2}{2}} du, \quad (20)$$

$$\begin{aligned} f_{\mathbf{Y}}(\mathbf{y}|\mathcal{H}_1) &= \frac{e^{-\frac{1}{2}\mathbf{y}^T\mathbf{R}^{-1}\mathbf{y} + \frac{C_2^2}{4C_1^2}}}{(2\pi)^{\frac{N_T}{2}}|\mathbf{R}|^{\frac{1}{2}}\sigma_t^2 C_1^2} \\ &\times \left(-\frac{1}{2} e^{-(\frac{C_2}{2C_1})^2} + \frac{\sqrt{\pi} C_2}{2C_1} Q(-\frac{C_2}{\sqrt{2} C_1}) \right) \\ &= \frac{e^{-\frac{1}{2}\mathbf{y}^T\mathbf{R}^{-1}\mathbf{y}}}{2(2\pi)^{\frac{N_T}{2}}|\mathbf{R}|^{\frac{1}{2}}\sigma_t^2 C_1^2} \\ &\times \left(1 + \frac{\sqrt{\pi} C_2}{C_1} e^{\frac{C_2^2}{4C_1^2}} Q(-\frac{C_2}{\sqrt{2} C_1}) \right). \end{aligned} \quad (21)$$

The likelihood ratio is defined as below. The detection is done by comparing this ratio with a determined threshold:

$$L(\mathbf{y}) = \frac{f_{\mathbf{Y}}(\mathbf{y}|\mathcal{H}_1)}{f_{\mathbf{Y}}(\mathbf{y}|\mathcal{H}_0)} = \frac{1}{2\sigma_t^2 C_1^2} \left(1 + \frac{\sqrt{\pi} C_2}{C_1} e^{\frac{C_2^2}{4C_1^2}} Q(-\frac{C_2}{\sqrt{2} C_1}) \right). \quad (22)$$

If $L(\mathbf{y})$ is greater than the threshold, hypothesis $\mathcal{H}_1$ is chosen, otherwise $\mathcal{H}_0$:

$$L(\mathbf{y}) \gtrless \eta_1. \quad (23)$$

Since $L(\mathbf{y})$ is a monotonically increasing function of C_2, the previous comparison can be replaced by the following comparison:

$$C_2 \gtrless \eta. \quad (24)$$

Here, we assume $\mathbf{R}$ is symmetric (it is a simplification assumption that is consistent with the situations we will consider in the simulations section), i.e.:

$$\mathbf{R}^T = \mathbf{R}. \quad (25)$$

Therefore, we have:

$$C_2 = \mathbf{s}^T\mathbf{R}^{-1}\mathbf{y} \gtrless \eta. \quad (26)$$

Subsequently, we define:

$$\mathbf{v} \triangleq \mathbf{R}^{-1}\mathbf{s}. \quad (27)$$

As a result:

$$C_2 = \mathbf{v}^T\mathbf{y} = \Sigma_{i=1}^{N_T} v_i y_i \gtrless \eta. \quad (28)$$

This is the structure of a filter (similar to the matched

filter) matched to $\mathbf{v}$. Now, we can compute P_{fa}:

$$T \triangleq \Sigma_{i=1}^{N_T} v_i y_i = \mathbf{v}^T \mathbf{y}. \quad (29)$$

Under the assumption of $\mathcal{H}_0$, T is a linear combination of N_T Gaussian variables. Therefore, it is Gaussian too and its mean and variance can be obtained as follows:

$$E\{T|\mathcal{H}_0\} = E\{\mathbf{v}^T\mathbf{y}|\mathcal{H}_0\} = \mathbf{v}^T E\{\mathbf{y}|\mathcal{H}_0\}$$
$$= E\{\mathbf{n}\} = 0, \quad (30)$$

$$var\{T|\mathcal{H}_0\} = E\{T^2|\mathcal{H}_0\} = E\{\mathbf{v}^T\mathbf{y}\ \mathbf{y}^T\mathbf{v}|\mathcal{H}_0\}$$
$$= \mathbf{v}^T E\{\mathbf{y}\mathbf{y}^T|\mathcal{H}_0\}\mathbf{v} = \mathbf{v}^T\mathbf{R}\mathbf{v}$$
$$= (\mathbf{R}^{-1}\mathbf{s})^T\mathbf{R}(\mathbf{R}^{-1}\mathbf{s}) = \mathbf{s}^T\mathbf{R}^{-1}\mathbf{R}\mathbf{R}^{-1}\ \mathbf{s}$$
$$= \mathbf{s}^T\mathbf{R}^{-1}\mathbf{s}. \quad (31)$$

So under the assumption of the hypothesis $\mathcal{H}_0$, T has the following distribution:

$$T|\mathcal{H}_0 \sim \mathcal{N}(0, \mathbf{s}^T\mathbf{R}^{-1}\mathbf{s}). \quad (32)$$

The probability of a false alarm can be computed as:

$$P_{fa} = \Pr\{T > \eta|\mathcal{H}_0\} = Q(\frac{\eta}{\sqrt{\mathbf{s}^T\mathbf{R}^{-1}\mathbf{s}}}). \quad (33)$$

If:

$$P_{fa} = \alpha, \quad (34)$$

then:

$$\eta = \sqrt{\mathbf{s}^T\mathbf{R}^{-1}\mathbf{s}}Q^{-1}(\alpha), \quad (35)$$

where η is the detector's threshold, which is determined according to the desired P_{fa} from the above equation.

Now, the probability of detection is computed under the assumption of $\mathcal{H}_1$:

$$T|\mathcal{H}_1 = \mathbf{v}^T\mathbf{y}|\mathcal{H}_1 = \mathbf{v}^T(\mathbf{n} + l\mathbf{s}) = \mathbf{v}^T\mathbf{n} + l\mathbf{v}^T\mathbf{s}. \quad (36)$$

For this n'th receiver, the probability of detecting the signal emitted by the m'th transmitter and then reflected by the target can be computed as follows:

$$P_d^{mn} = \Pr\{T > \eta|\mathcal{H}_1\} = \Pr\{\mathbf{v}^T\mathbf{n} + l\mathbf{v}^T\mathbf{s} > \eta\}$$
$$= \int_0^\infty \Pr\{\mathbf{v}^T\mathbf{n} > \eta - \mathbf{v}^T\mathbf{s}x\} f_L(x)dx. \quad (37)$$

From Eq. (27), we have:

$$\Pr\{\mathbf{v}^T\mathbf{n} > \eta - \mathbf{v}^T\mathbf{s}x\} = Q(\frac{\eta - \mathbf{v}^T\mathbf{s}x}{\sqrt{\mathbf{s}^T\mathbf{R}^{-1}\mathbf{s}}}), \quad (38)$$

$$\mathbf{v}^T\mathbf{s} = \mathbf{s}^T\mathbf{R}^{-1}\mathbf{s}, \quad (39)$$

$$\Pr\{\mathbf{v}^T\mathbf{n} > \eta - \mathbf{v}^T\mathbf{s}x\} = Q(\frac{\eta - \mathbf{s}^T\mathbf{R}^{-1}\mathbf{s}x}{\sqrt{\mathbf{s}^T\mathbf{R}^{-1}\mathbf{s}}}). \quad (40)$$

From Eqs. (37) and (39), we can write:

$$P_d^{mn} = \int_0^\infty Q\left(\frac{\eta - \mathbf{s}^T\mathbf{R}^{-1}\mathbf{s}x}{\sqrt{\mathbf{s}^T\mathbf{R}^{-1}\mathbf{s}}}\right)\frac{x}{\sigma_t^2}e^{-\frac{x^2}{2\sigma_t^2}}dx. \quad (41)$$

Substituting the threshold from Eq. (35):

$$P_d^{mn} = \int_0^\infty Q(Q^{-1}(\alpha) - \sqrt{\mathbf{s}^T\mathbf{R}^{-1}\mathbf{s}}x)\frac{x}{\sigma_t^2}e^{-\frac{x^2}{2\sigma_t^2}}dx$$
$$= \int_0^\infty \left(1 - Q(\sqrt{\mathbf{s}^T\mathbf{R}^{-1}\mathbf{s}}x - Q^{-1}(\alpha))\right)\frac{x}{\sigma_t^2}e^{-\frac{x^2}{2\sigma_t^2}}dx$$
$$= \int_0^\infty \frac{x}{\sigma_t^2}e^{-\frac{x^2}{2\sigma_t^2}}dx$$
$$- \int_0^\infty Q\left(\sqrt{\mathbf{s}^T\mathbf{R}^{-1}\mathbf{s}}x - Q^{-1}(\alpha)\right)\frac{x}{\sigma_t^2}e^{-\frac{x^2}{2\sigma_t^2}}dx$$
$$= 1 - \int_0^\infty Q(\sqrt{\mathbf{s}^T\mathbf{R}^{-1}\mathbf{s}}x - Q^{-1}(\alpha))\frac{x}{\sigma_t^2}e^{-\frac{x^2}{2\sigma_t^2}}dx, \quad (42)$$

$$P_{\text{miss}}^{mn} = 1 - P_d^{mn} = \int_0^\infty Q\left(\sqrt{\mathbf{s}^T\mathbf{R}^{-1}\mathbf{s}}x - Q^{-1}(\alpha)\right)$$
$$\times \frac{x}{\sigma_t^2}e^{-\frac{x^2}{2\sigma_t^2}}dx, \quad (43)$$

$$u \triangleq \frac{x^2}{2\sigma_t^2}, \quad (44)$$

$$P_{\text{miss}}^{mn} = \int_0^\infty Q(\sqrt{\mathbf{s}^T\mathbf{R}^{-1}\mathbf{s}}\sigma_t\sqrt{2u} - Q^{-1}(\alpha))e^{-u}du, \quad (45)$$

$$A \triangleq \sigma_t\sqrt{2\mathbf{s}^T\mathbf{R}^{-1}\mathbf{s}}, \quad (46)$$

$$B \triangleq Q^{-1}(\alpha), \quad (47)$$

$$P_{\text{miss}}^{mn} = \int_0^\infty Q(A\sqrt{u} - B)e^{-u}du$$
$$= \int_0^\infty \left(\int_{A\sqrt{u}-B}^\infty \frac{1}{\sqrt{2\pi}}e^{-\frac{t^2}{2}}dt\right)e^{-u}du, \quad (48)$$

$$t > A\sqrt{u} - B \Rightarrow \frac{t+B}{A} > \sqrt{u} \Rightarrow (\frac{t+B}{A})^2 > u. \quad (49)$$

We can rewrite the probability of missed detection by

displacing the bounds of the two integrals as:

$$\begin{aligned}P_{\text{miss}}^{mn} &= \frac{1}{\sqrt{2\pi}}\int_{-B}^{\infty} e^{-\frac{t^2}{2}}dt\int_{0}^{(\frac{t+B}{A})^2} e^{-u}du\\ &= \frac{1}{\sqrt{2\pi}}\int_{-B}^{\infty} e^{-\frac{t^2}{2}}(1-e^{-(\frac{t+B}{A})^2})dt\\ &= Q(-B)-\frac{1}{\sqrt{2\pi}}e^{-\frac{B^2}{A^2}}\int_{-B}^{\infty} e^{-\frac{t^2(A^2+2)}{2A^2}-\frac{2tB}{A^2}}dt\\ &= Q(-B)-\frac{1}{\sqrt{2\pi}}e^{-\frac{B^2}{A^2}+\frac{2B^2}{A^2(A^2+2)}}\\ &\times\int_{-B}^{\infty} e^{-(\frac{t}{A}\sqrt{\frac{A^2+2}{2}}+\frac{B\sqrt{2}}{A\sqrt{A^2+2}})^2}dt\\ &= Q(-B)-\frac{1}{\sqrt{2\pi}}e^{-\frac{B^2}{A^2}+\frac{2B^2}{A^2(A^2+2)}}\sqrt{\frac{A^2}{A^2+2}}\\ &\times\int_{-\frac{B}{A}\sqrt{A^2+2}+\frac{2B}{A\sqrt{A^2+2}}}^{\infty} e^{-\frac{t'^2}{2}}dt'\\ &= Q(-B)-\sqrt{\frac{A^2}{A^2+2}}e^{\frac{-B^2}{A^2+2}}\\ &\times Q\left(\frac{B}{A}\left(\sqrt{\frac{4}{A^2+2}}-\sqrt{A^2+2}\right)\right).\end{aligned} \tag{50}$$

Here, we have substituted B and have used the property of the Q-function:

$$Q(-B)=1-Q(B)=1-Q(Q^{-1}(\alpha))=1-\alpha, \tag{51}$$

$$\begin{aligned}P_{\text{miss}}^{mn} &= 1-\alpha-\sqrt{\frac{k^2}{k^2+1}}e^{-\frac{(Q^{-1}(\alpha))^2}{2(k^2+1)}}\\ &\times Q\left(\frac{Q^{-1}(\alpha)}{\sqrt{2}k}\left(\sqrt{\frac{2}{k^2+1}}-\sqrt{2(k^2+1)}\right)\right)\\ &= 1-\alpha-\sqrt{\frac{k^2}{k^2+1}}e^{-\frac{(Q^{-1}(\alpha))^2}{2(k^2+1)}}\\ &\times Q\left(\frac{Q^{-1}(\alpha)}{k\sqrt{k^2+1}}(1-(k^2+1))\right)\\ &= 1-\alpha-\sqrt{\frac{k^2}{k^2+1}}e^{-\frac{(Q^{-1}(\alpha))^2}{2(k^2+1)}}\\ &\times Q\left(\frac{-k}{\sqrt{k^2+1}}Q^{-1}(\alpha)\right),\end{aligned} \tag{52}$$

where:

$$k^2=\frac{A^2}{2}=\sigma_t^2\mathbf{s}^T\mathbf{R}^{-1}\mathbf{s}. \tag{53}$$

If we define:

$$d^{mn}\triangleq-\lim_{SNR\to\infty}\frac{\log P_{\text{miss}}^{mn}}{\log \text{SNR}}, \tag{54}$$

we will deduce (from Eqs. (2) and (5)):

$$d_{\text{total}}=\Sigma_{m=1}^{M}\Sigma_{n=1}^{N}d^{mn}. \tag{55}$$

Here, by defining the SNR as the ratio of the detector's output in the case of $\mathcal{H}_1$ to the detector's output in the case of $\mathcal{H}_0$, we have:

$$\begin{aligned}\text{SNR} &= \frac{E\{T^2|\mathbf{y}=l\mathbf{s}\}}{E\{T^2|\mathbf{y}=\mathbf{n}\}}=\frac{E\{(l\mathbf{v}^T\mathbf{s})^2\}}{E\{\mathbf{v}^T\mathbf{n}\mathbf{n}^T\mathbf{v}\}}\\ &= \frac{(\mathbf{v}^T\mathbf{s})^2E\{l^2\}}{\mathbf{v}^T\mathbf{R}\mathbf{v}}=\frac{(\mathbf{s}^T\mathbf{R}^{-1}\mathbf{s})^2\sigma_t^2}{\mathbf{s}^T\mathbf{R}^{-1}\mathbf{s}}=\sigma_t^2\mathbf{s}^T\mathbf{R}^{-1}\mathbf{s},\end{aligned} \tag{56}$$

$$k^2=\text{SNR}, \tag{57}$$

$$\begin{aligned}\lim_{\text{SNR}\to\infty}P_{\text{miss}}^{mn} &= \lim_{k\to\infty}P_{\text{miss}}^{mn}=\lim_{k\to\infty}1-\alpha\\ &-\sqrt{\frac{k^2}{k^2+1}}e^{-\frac{(Q^{-1}(\alpha))^2}{2(k^2+1)}}Q\left(\frac{-k}{\sqrt{k^2+1}}Q^{-1}(\alpha)\right),\end{aligned} \tag{58}$$

$$\lim_{k\to\infty}\sqrt{\frac{k^2}{k^2+1}}=\lim_{k\to\infty}1-\frac{1}{2k^2}+o(\frac{1}{k^2}), \tag{59}$$

where the definition of $o(.)$ comes from:

$$f(x)=o(g(x))\Leftrightarrow\lim_{x\to\infty}\frac{f(x)}{g(x)}=0, \tag{60}$$

$$\lim_{k\to\infty}e^{-\frac{(Q^{-1}(\alpha))^2}{2(k^2+1)}}=\lim_{k\to\infty}1-\frac{(Q^{-1}(\alpha))^2}{2k^2}+o(\frac{1}{k^2}). \tag{61}$$

Using the Taylor series of the Q-function, we have:

$$Q(x_0+\delta)=Q(x_0)+\delta Q'(x_0)+o(\delta), \tag{62}$$

$$\begin{aligned}Q'(x_0) &= \frac{d}{dx}\int_{x}^{\infty}\frac{1}{\sqrt{2\pi}}e^{-\frac{t^2}{2}}dt|_{x=x_0}\\ &= -\frac{1}{\sqrt{2\pi}}e^{-\frac{x^2}{2}}|_{x=x_0}=-\frac{1}{\sqrt{2\pi}}e^{-\frac{x_0^2}{2}},\end{aligned} \tag{63}$$

$$Q(x_0+\delta)=Q(x_0)-\delta\frac{1}{\sqrt{2\pi}}e^{-\frac{x_0^2}{2}}+o(\delta), \tag{64}$$

From Eq. (64), we can write:

$$\lim_{k\to\infty} Q\left(\frac{-k}{\sqrt{k^2+1}}Q^{-1}(\alpha)\right) = Q\left(-\sqrt{\frac{k^2}{k^2+1}}Q^{-1}(\alpha)\right) = Q(-Q^{-1}(\alpha)(1-\frac{1}{2k^2}+o(\frac{1}{k^2}))) = Q(-Q^{-1}(\alpha)) - \frac{1}{2k^2}Q^{-1}(\alpha)\frac{1}{\sqrt{2\pi}}e^{-\frac{(Q^{-1}(\alpha))^2}{2}} + o(\frac{1}{k^2}) = 1-\alpha-\frac{1}{2k^2}Q^{-1}(\alpha)\frac{1}{\sqrt{2\pi}}e^{-\frac{(Q^{-1}(\alpha))^2}{2}} + o(\frac{1}{k^2}). \quad (65)$$

Using Eqs. (59), (61) and (65), we can write the following for the probability of missed detection:

$$\lim_{k\to\infty} P_{\text{miss}}^{mn} = 1-\alpha-\left(1-\frac{1}{2k^2}+o(\frac{1}{k^2})\right) \times \left(1-\frac{(Q^{-1}(\alpha))^2}{2k^2}+o(\frac{1}{k^2})\right) \times \left(1-\alpha-\frac{1}{2k^2}Q^{-1}(\alpha)\frac{1}{\sqrt{2\pi}}e^{-\frac{(Q^{-1}(\alpha))^2}{2}}+o(\frac{1}{k^2})\right) = 1-\alpha-\left(1-\frac{1+(Q^{-1}(\alpha))^2}{2k^2}\right) \times \left(1-\alpha-\frac{1}{2k^2}Q^{-1}(\alpha)\frac{1}{\sqrt{2\pi}}e^{-\frac{(Q^{-1}(\alpha))^2}{2}}+o(\frac{1}{k^2})\right) = (1-\alpha)\frac{1+(Q^{-1}(\alpha))^2}{2k^2} + \frac{1}{2k^2}Q^{-1}(\alpha)\frac{1}{\sqrt{2\pi}}e^{-\frac{(Q^{-1}(\alpha))^2}{2}}+o(\frac{1}{k^2}) = \frac{1}{2k^2}((1-\alpha)(1+(Q^{-1}(\alpha))^2) + \frac{1}{\sqrt{2\pi}}Q^{-1}(\alpha)e^{-\frac{(Q^{-1}(\alpha))^2}{2}}), \quad (66)$$

$$\lim_{\text{SNR}\to\infty} \log P_{\text{miss}}^{mn} = \log\left(\frac{1}{2}\left((1-\alpha)(1+(Q^{-1}(\alpha))^2) + \frac{1}{\sqrt{2\pi}}Q^{-1}(\alpha)e^{-\frac{(Q^{-1}(\alpha))^2}{2}}\right)\right) - \log(\text{SNR}), \quad (67)$$

$$d^{mn} = -\lim_{\text{SNR}\to\infty}\frac{\log P_{\text{miss}}^{mn}}{\log \text{SNR}} = 1. \quad (68)$$

Therefore:

$$d_{\text{total}} = \Sigma_{m=1}^{M}\Sigma_{n=1}^{N} d^{mn} = MN. \quad (69)$$

As can be observed, in the MIMO passive coherent location, specifically in a single frequency network, the spatial diversity gain is proportional to the product of the number of transmit antennas and the receive antennas.

3. Simulations

In this section, DVB-T stations are used as the non-cooperative illuminators of opportunity, and the DVB-T signal has the same properties as those used in [6]. Also, four different cases for the covariance matrix ($\mathbf{R}$) are assumed:

1. White gaussian noise;
2. Colored noise;
3. Clutter;
4. Clutter plus white noise.

In order to verify the results of the previous section, for each case, P_{miss} vs SNR is depicted for different numbers of antennas at the receive and transmit sides using the Monte-Carlo method.

3.1. White Gaussian noise

When the only interference is white noise, we have:

$$\mathbf{R} = \sigma_n^2 I. \quad (70)$$

For this case, the detector structure is:

$$T = \mathbf{s}^T\mathbf{R}^{-1}\mathbf{y} \gtrless \eta, \quad (71)$$

$$\mathbf{s}^T\mathbf{y} \gtrless \eta' = \eta\sigma_n^2, \quad (72)$$

which is the structure of a matched filter:

$$P_{fa} = Q(\frac{\eta}{\sqrt{\mathbf{s}^T\mathbf{R}^{-1}\mathbf{s}}}) = Q(\frac{\sigma_n\eta}{\sqrt{\mathbf{s}^T\mathbf{s}}}), \quad (73)$$

$$P_{fa} = \alpha, \quad (74)$$

$$\eta = \frac{\sqrt{\mathbf{s}^T\mathbf{s}}}{\sigma_n}Q^{-1}(\alpha), \quad (75)$$

$$\eta' = \sigma_n\sqrt{\mathbf{s}^T\mathbf{s}}Q^{-1}(\alpha), \quad (76)$$

$$k^2 = \sigma_t^2\mathbf{s}^T\mathbf{R}^{-1}\mathbf{s} = \frac{\sigma_t^2}{\sigma_n^2}\mathbf{s}^T\mathbf{s}. \quad (77)$$

The resulting P_{miss} is shown in Figure 2. The diversity gain achieved by increasing the number of antennas of

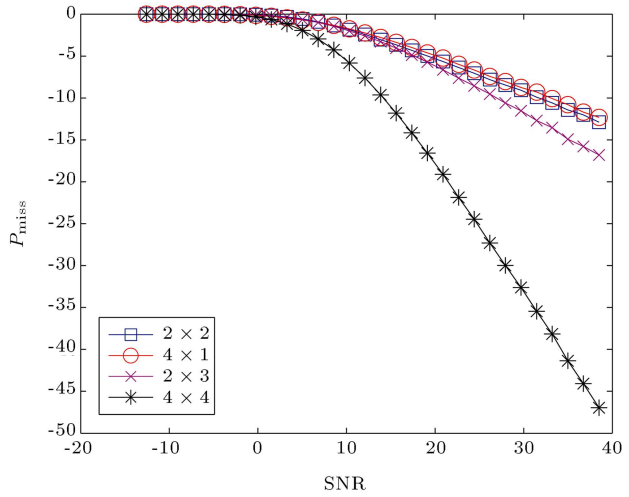

Figure 2. Detection performance for the case of white noise.

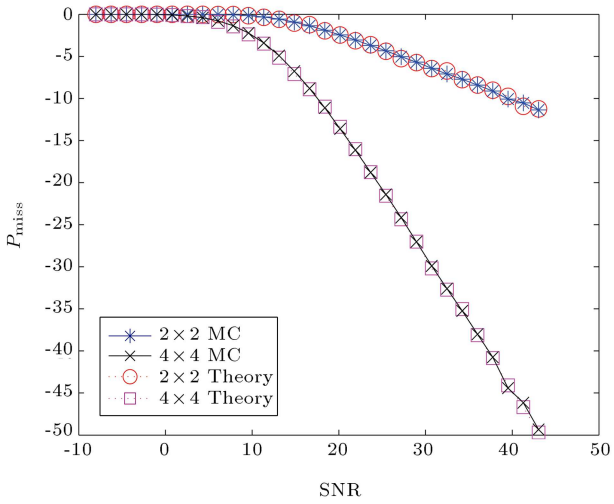

Figure 3. Detection performance for the case of colored noise.

the MIMO configuration is obvious. Also, as expected from the theoretical results of the previous section, the diversity gain of the two configurations of 'two transmitters and two receivers' (2×2) should be equal to the diversity gain of the case of 'four transmitters and one receiver' (4×1). This fact is verified in Figure 2, where the slope of the two lines corresponding to the two aforementioned cases are the same at high SNRs.

3.2. Colored noise

In the case of colored noise that we assume here, the noise samples are independent but have different energies. So:

$$\mathbf{R} = \text{diag}\left(\sigma_1^2, \sigma_2^2, \ldots, \sigma_{N_T}^2\right),$$

$$\mathbf{R}^{-1} = \text{diag}\left(\frac{1}{\sigma_1^2}, \frac{1}{\sigma_2^2}, \ldots, \frac{1}{\sigma_{N_T}^2}\right),$$

$$\mathbf{s}^T\mathbf{R}^{-1} = \left[\frac{s_1}{\sigma_1^2}, \frac{s_2}{\sigma_2^2}, \ldots, \frac{s_{N_T}}{\sigma_{N_T}^2}\right], \tag{78}$$

$$T = \Sigma_{i=1}^{N_T} \frac{1}{\sigma_i^2} s_i y_i \gtrless \eta, \tag{79}$$

which is a filter matched to $\mathbf{v} = \left[\frac{s_1}{\sigma_1^2}, \frac{s_2}{\sigma_2^2}, \ldots, \frac{s_{N_T}}{\sigma_{N_T}^2}\right]^T$:

$$\sqrt{\mathbf{s}^T\mathbf{R}^{-1}\mathbf{s}} = \sqrt{\Sigma_{i=1}^{N_T} \frac{s_i^2}{\sigma_i^2}}, \tag{80}$$

$$P_{fa} = Q\left(\frac{\eta}{\sqrt{\Sigma_{i=1}^{N_T} \frac{s_i^2}{\sigma_i^2}}}\right), \tag{81}$$

$$P_{fa} = \alpha, \tag{82}$$

$$\eta = Q^{-1}(\alpha)\sqrt{\Sigma_{i=1}^{N_T} \frac{s_i^2}{\sigma_i^2}}, \tag{83}$$

$$k^2 = \sigma_t^2 \mathbf{s}^T\mathbf{R}^{-1}\mathbf{s} = \sigma_t^2 \Sigma_{i=1}^{N_T} \frac{s_i^2}{\sigma_i^2}. \tag{84}$$

The results are depicted in Figure 3. As can be easily verified, they are consistent with the expected theoretical results.

3.3. Clutter

In this case, the covariance matrix is as given below:

$$\mathbf{R} = \sigma_c^2 \begin{bmatrix} 1 & \rho & \ldots & \rho^{N_T-1} & \rho^{N_T} \\ \rho & 1 & \ldots & \rho^{N_T-2} & \rho^{N_T-1} \\ . & . & \ldots & . & . \\ . & . & \ldots & . & . \\ \rho^{N_T-1} & \rho^{N_T-2} & \ldots & 1 & \rho \\ \rho^{N_T} & \rho^{N_T-1} & \ldots & \rho & 1 \end{bmatrix}, \tag{85}$$

where σ_c is the power of the clutter.

The interpretation of the above formula is that the correlation between the samples reduces proportional to ρ ($0 < \rho < 1$) as their distance increases. As ρ becomes smaller, the signal becomes more stochastic (becomes more similar to white noise, e.g. $\rho = 0$ corresponds to the white noise case), and, as it grows, the signal becomes more similar to clutter only ($\rho = 1$ corresponds to the covariance matrix of the clutter).

Here, the covariance matrix ($\mathbf{R}$) is Toeplitz, which results in:

$$\mathbf{R}^{-1} = \frac{1}{\sigma_c^2(1-\rho^2)}$$

$$\times \begin{bmatrix} 1 & -\rho & 0 & \dots & 0 & 0 \\ -\rho & 1+\rho^2 & -\rho & \dots & 0 & 0 \\ 0 & -\rho & 1+\rho^2 & \dots & 0 & 0 \\ . & . & . & \dots & . & . \\ . & . & . & \dots & . & . \\ 0 & 0 & 0 & \dots & 1+\rho^2 & -\rho \\ 0 & 0 & 0 & \dots & -\rho & 1 \end{bmatrix}. \quad (86)$$

After suppressing the energy of clutter using the canceller at the input of the detector, its power (σ_c) will be comparable to the noise power. In the simulations, σ_c is chosen 1.5 times the power of noise. Also, we have chosen $\rho = 0.9$ for the clutter.

$$\mathbf{v} = \mathbf{R}^{-1}\mathbf{s} = \frac{1}{\sigma_c^2(1-\rho^2)} \begin{bmatrix} s_1 - \rho s_2 \\ -\rho s_1 + (1+\rho^2)s_2 - \rho s_3 \\ . \\ . \\ . \\ -\rho s_{N_T-2} + (1+\rho^2)s_{N_T-1} - \rho s_{N_T} \\ -\rho s_{N_T-1} + s_{N_T} \end{bmatrix}. \quad (87)$$

Therefore, the filter should be matched to the $\mathbf{v}$ of Eq. (87):

$$T = \mathbf{v}^T\mathbf{y} = \frac{1}{\sigma_c^2(1-\rho^2)} \Big[(s_1 - \rho s_2) y_1 + \sum_{i=1}^{N_T-2} \left(-\rho s_i + (1+\rho^2)s_{i+1} - \rho s_{i+2}\right) y_{i+1} + \left(-\rho s_{N_T-1} + s_{N_T}\right) y_{N_T} \Big] \gtrless \eta. \quad (88)$$

It can be shown that:

$$T = \sum_{k=1}^{N_T} b_k z_k \gtrless \eta, \quad (89)$$

where:

$$b_1 = \frac{s_1}{\sigma_c}, \quad b_k = \frac{s_k - \rho s_{k-1}}{\sigma_c\sqrt{1-\rho^2}},$$
$$z_1 = \frac{y_1}{\sigma_c}, \quad z_k = \frac{y_k - \rho y_{k-1}}{\sigma_c\sqrt{1-\rho^2}}. \quad (90)$$

In order to compute P_{fa}, we have:

$$\mathbf{s}^T\mathbf{R}^{-1}\mathbf{s} = \sum_{k=1}^{N_T} b_k^2 = (\frac{s_1}{\sigma_c})^2 + \sum_{k=2}^{N_T} \frac{(s_k - \rho s_{k-1})^2}{\sigma_c^2(1-\rho^2)}, \quad (91)$$

$$P_{fa} = Q(\frac{\eta}{\sum_{k=1}^{N_T} b_k^2}) \Rightarrow \eta = Q^{-1}(\alpha)\sum_{k=1}^{N_T} b_k^2$$

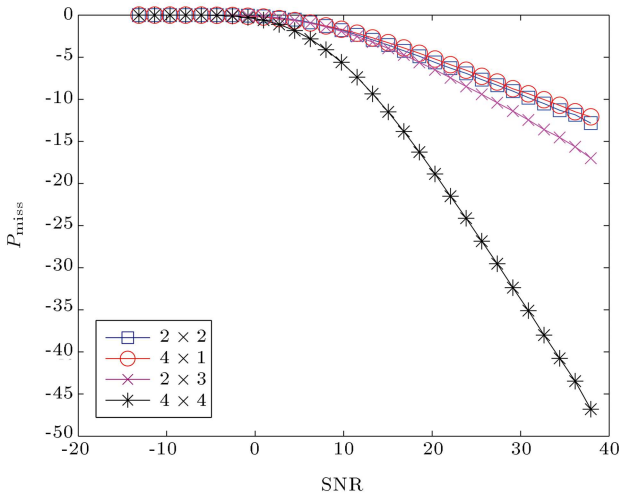

Figure 4. Detection performance for the case of clutter.

$$= Q^{-1}(\alpha)\left[(\frac{s_1}{\sigma_c})^2 + \sum_{k=2}^{N_T}\left(\frac{s_k - \rho s_{k-1}}{\sigma_c\sqrt{1-\rho^2}}\right)^2\right], \quad (92)$$

$$k^2 = \sigma_t^2\mathbf{s}^T\mathbf{R}^{-1}\mathbf{s} = \sigma_t^2\Sigma_{i=1}^{N_T} b_i^2 = \sigma_t^2\left((\frac{s_1}{\sigma_c})^2 + \Sigma_{i=2}^{N_T}\frac{(s_i - \rho s_{i-1})^2}{\sigma_c^2(1-\rho^2)}\right). \quad (93)$$

Figure 4 shows the detector's probability of missed detection for this case. Again, the expected diversity gain is achieved by using multiple antennas in a MIMO configuration.

3.4. Clutter plus white noise

In this case:

$$R = \sigma_n^2 I + \sigma_c^2 \times \begin{bmatrix} 1 & \rho & \dots & \rho^{N_T-1} & \rho^{N_T} \\ \rho & 1 & \dots & \rho^{N_T-2} & \rho^{N_T-1} \\ . & . & \dots & . & . \\ . & . & \dots & . & . \\ \rho^{N_T-1} & \rho^{N_T-2} & \dots & 1 & \rho \\ \rho^{N_T} & \rho^{N_T-1} & \dots & \rho & 1 \end{bmatrix}, \quad (94)$$

$$R = \begin{bmatrix} \sigma_n^2+\sigma_c^2 & \sigma_c^2\rho & \dots & \sigma_c^2\rho^{N_T-1} & \sigma_c^2\rho^{N_T} \\ \sigma_c^2\rho & \sigma_n^2+\sigma_c^2 & \dots & \sigma_c^2\rho^{N_T-2} & \sigma_c^2\rho^{N_T-1} \\ . & . & \dots & . & . \\ . & . & \dots & . & . \\ \sigma_c^2\rho^{N_T-1} & \sigma_c^2\rho^{N_T-2} & \dots & \sigma_n^2+\sigma_c^2 & \sigma_c^2\rho \\ \sigma_c^2\rho^{N_T} & \sigma_c^2\rho^{N_T-1} & \dots & \sigma_c^2\rho & \sigma_n^2+\sigma_c^2 \end{bmatrix}. \quad (95)$$

The earlier assumptions are considered for σ_c, but,

$$R^{-1} = \frac{1}{\sigma_c^2(a^2+(N_T-2)a-(N_T-1)}) \begin{bmatrix} a+N_T-2 & -1 & \dots & -1 & -1 \\ -1 & a+N_T-2 & \dots & -1 & -1 \\ . & . & \dots & . & . \\ . & . & \dots & . & . \\ -1 & -1 & \dots & a+N_T-2 & -1 \\ -1 & -1 & \dots & -1 & a+N_T-2 \end{bmatrix}, \quad (96)$$

where:

$$a = \frac{\sigma_n^2+\sigma_c^2}{\sigma_c^2}, \quad (97)$$

$$\sigma_c^2(a^2+(N_T-2)a-(N_T-1))v_i = (a+N_T-2)s_i - \sum_{j=1,i\neq j}^{N_T} s_i = (a+N_T-1)s_i - \sum_{j=1}^{N_T} s_j. \quad (98)$$

Box I

here, by setting ρ to 1, we will have Eq. (96) shown in Box I.

The filter should be matched to $\mathbf{v}$, where it is computed as below:

$$\mathbf{v} = \left((a+N_T-1)\mathbf{s} - \begin{bmatrix} 1 & 1 & \dots & 1 \end{bmatrix}^T \sum_{j=1}^{N_T} s_j \right) \times \frac{1}{\sigma_c^2\left(a^2+(N_T-2)a-(N_T-1)\right)}. \quad (99)$$

If we define:

$$G^2 \triangleq \mathbf{s}^T R^{-1}\mathbf{s} = \left((a+N_T-1)\mathbf{s}^T\mathbf{s} - (\sum_{j=1}^{N_T} s_j)^2 \right) \times \frac{1}{\sigma_c^2(a^2+(N_T-2)a-(N_T-1))}, \quad (100)$$

we will have:

$$P_{fa} = Q(\frac{\eta}{G}) \Rightarrow \eta = GQ^{-1}(\alpha)$$

$$\Rightarrow \eta = \sqrt{\frac{(a+N_T-1)\mathbf{s}^T\mathbf{s} - (\sum_{j=1}^{N_T} s_j)^2}{\sigma_c^2(a^2+(N_T-2)a-(N_T-1))}}, \quad (101)$$

$$k^2 = \sigma_t^2 \mathbf{s}^T \mathbf{R}^{-1}\mathbf{s} = \sigma_t^2 G^2. \quad (102)$$

The detector's performance for different numbers of antenna at the transmit and receive sides is shown in Figure 5. It verifies that using more antennas gives better performance at high SNRs. In addition, in order to verify the theoretical results derived in the previous section, we have compared the Monte-Carlo simulations with the theoretical results of P_{miss} for the case of 2×2 and 4×4 configurations in Figure 6.

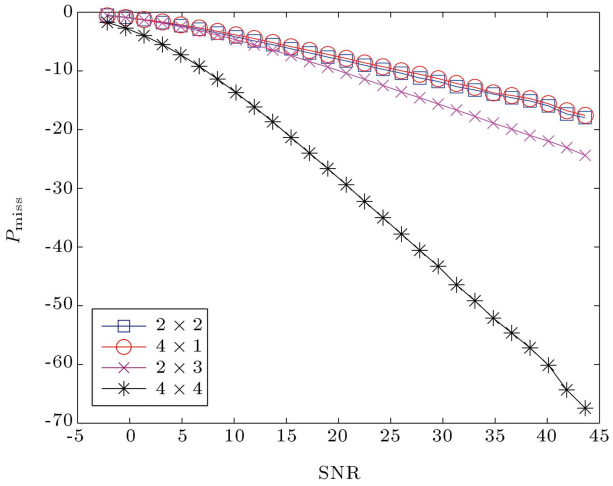

Figure 5. Detection performance for the case of clutter plus white noise.

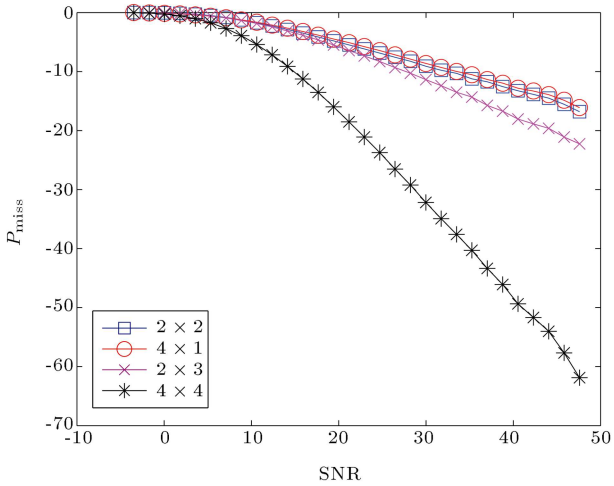

Figure 6. The theoretical results vs the simulation's results.

4. Conclusion

In the Passive Coherent Location (PCL), the objects are detected and localized by the illuminators of opportunity already present in the environment. The idea of using multiples of these noncooperative transmitters and doing the detection by multiple receive antennas is expected to bring us the advantages of the so-called MIMO systems. An important aspect of such systems is obtaining a spatial diversity gain proportional to the product of the number of transmit and receive antennas. Obtaining this gain was already shown in recent research for the case of active transmitters, where the transmit antennas are under control. However, this is not the case when using the illuminators of opportunity of a single frequency network, such as DVB-T. Although such a network is quite interesting for use in a MIMO configuration, transmission of the same signal from all transmitters can degrade the efficiency of the MIMO system. The concern arises from recent observations on active transmitters, in which the assumption of sending orthogonal signals, in order to separate them at the receive side, plays a fundamental role in obtaining spatial diversity. In this paper, we show that even in a MIMO PCL working under SFN conditions, the diversity gain of other common MIMO systems can still be obtained.

References

1. Howland, P. "Editorial", *Passive Radar Systems*, **152**(3), pp. 105-106 (2005).
2. Howland, P., Maksimiuk, D. and Reitsma, G. "FM radio based bistatic radar", *IEE Proceedings-Radar, Sonar and Navigation*, **152**(3), pp. 107-115 (2005).
3. Griffiths, H. and Long, N. "Television-based bistatic radar", *IEE Proceedings F- Communications, Radar and Signal Processing*, **133**(7), pp. 649-657 (2008).
4. Howland, P. "Target tracking using television-based bistatic radar", *IEE Proceedings-Radar, Sonar and Navigation*, **146**(3), pp. 166-174 (2002).
5. Coleman, C., Watson, R., Yardley, H., Coleman, C.J., Watson, R.A. and Yardley, H.A. "Practical bistatic passive radar system for use with DAB and DRM illuminators", In *IEEE Radar Conference* (2008).
6. Radmard, M., Bastani, M., Behnia, F., Radmard, M., Bastani, M. and Behnia, F. "Cross ambiguity function analysis of the '8k-mode' DVB-T for passive radar application", In *IEEE Radar Conference* (2010).
7. Saini, R. and Cherniakov, M. "DTV signal ambiguity function analysis for radar application", *IEE Proceedings-Radar, Sonar and Navigation*, **152**(3), pp. 133-142 (2005).
8. Griffiths, H., Garnett, A., Baker, C., Keaveney, S., Griffiths, H.D., Garnett, A.J., Baker, C.J. and Keaveney, S. "Bistatic radar using satellite-borne illuminators of opportunity", In *International Radar Conference* (2002).
9. Tan, D., Sun, H., Lu, Y., Lesturgie, M. and Chan, H. "Passive radar using global system for mobile communication signal: Theory, implementation and measurements", *IEE Proceedings - Radar, Sonar and Navigation*, **152**(3), pp. 116-123 (2005).
10. Sun, H., Tan, D., Lu, Y., Sun, H., Tan, D.K.P. and Lu, Y. "Aircraft target measurements using A GSM-based passive radar", In *IEEE Radar Conference* (2008).
11. Poullin, D. "Passive detection using digital broadcasters (DAB, DVB) with COFDM modulation", *IEE Proceedings - Radar, Sonar and Navigation*, **152**(3), pp. 143-152 (2005).
12. Daun, M., Koch, W., Daun, M. and Koch, W. "Multistatic target tracking for non-cooperative illuminating by DAB/DVB-T", In *OCEANS*, 2007-Europe (2007).
13. Daun, M. and Nickel, U. "Tracking in multistatic passive radar systems using DAB/DVB-T illumination", *Signal Processing* (2011).
14. Haimovich, A., Blum, R. and Cimini, L. "MIMO radar with widely separated antennas", *IEEE Signal Processing Magazine*, **25**(1), pp. 116-129 (2007).
15. Li, J. and Stoica, P. "MIMO radar with colocated antennas", *IEEE Signal Processing Magazine*, **24**(5), pp. 106-114 (2007).
16. Lehmann, N., Fishler, E., Haimovich, A., Blum, R., Chizhik, D., Cimini, L. and Valenzuela, R. "Evaluation of transmit diversity in MIMO-radar direction finding", *IEEE Transactions on Signal Processing*, **55**(5), pp. 2215-2225 (2007).
17. Fishler, E., Haimovich, A., Blum, R., Cimini Jr, L., Chizhik, D. and Valenzuela, R. "Spatial diversity in radars-models and detection performance", *IEEE Transactions on Signal Processing*, **54**(3), pp. 823-838 (2006).
18. De Maio, A. and Lops, M. "Design principles of MIMO radar detectors", *IEEE Transactions on Aerospace and Electronic Systems*, **43**(3), pp. 886-898 (2007).
19. Habtemariam, B., Tharmarasa, R., Kirubarajan, T., Habtemariam, B.K., Tharmarasa, R. and Kirubarajan, T. "Multitarget track before detect with MIMO radars", In *IEEE Aerospace Conference* (2010).
20. Fishler, E., Haimovich, A., Blum, R., Chizhik, D., Cimini, L., Valenzuela, R., Fishler, E., Haimovich, A., Blum, R., Chizhik, D., Cimini, L. and Valenzuela, R. "MIMO radar: An idea whose time has come", In *IEEE Radar Conference* (2004).
21. Li, J., Stoica, P., Xu, L. and Roberts, W. "On parameter identifiability of MIMO radar", *IEEE Signal Processing Letters*, **14**(12), pp. 968-971 (2007).
22. Yang, Y. and Blum, R. "MIMO radar waveform design based on mutual information and minimum mean-square error estimation", *IEEE Transactions on Aerospace and Electronic Systems*, **43**(1), pp. 330-343 (2007).

23. Xu, L., Li, J., Stoica, P., Xu, L., Li, J. and Stoica, P. "Radar imaging via adaptive MIMO techniques", In *Proc. 14th Eur. Signal Process. Conf.* (2006).

24. Wang, H., Liao, G., Liu, H., Li, J. and Lv, H. "Joint optimization of MIMO radar waveform and biased estimator with prior information in the presence of clutter", *EURASIP Journal on Advances in Signal Processing*, **2011**(1), p. 15 (2011).

25. Fuhrmann, D. and San Antonio, G. "Transmit beamforming for MIMO radar systems using signal cross-correlation", *IEEE Transactions on Aerospace and Electronic Systems*, **44**(1), pp. 171-186 (2008).

26. Stoica, P., Li, J. and Xie, Y. "On probing signal design for MIMO radar", *IEEE Transactions on Signal Processing*, **55**(8), pp. 4151-4161 (2007).

27. Lozano, N. and Jindal, A. "Transmit diversity vs. spatial multiplexing in modern MIMO systems", *IEEE Transactions on Wireless Communications*, **9**, pp. 186-197 (2010).

28. Goldsmith, A., *Wireless Communications*, Cambridge University Press (2005).

29. Tse, D. and Viswanath, P., *Fundamentals of Wireless Communication*, Cambridge University Press (2005).

30. Chernyak, V. and Chernyak, V.S. "On the concept of MIMO radar", In *IEEE Radar Conference* (2010).

31. He, Q., Blum, R. and Haimovich, A. "Noncoherent MIMO radar for location and velocity estimation: More antennas means betterperformance", *IEEE Transactions on Signal Processing*, **58**(7), pp. 3661-3680 (2010).

32. He, Q. and Blum, R. "Diversity gain for MIMO neyman-pearson signal detection", *IEEE Transactions on Signal Processing*, **59**(3), pp. 869-881 (2011).

33. Badrinath, S., Srinivas, A. and Reddy, V. "Low-complexity design of frequency-hopping codes for MIMO radar for arbitrary Doppler", *EURASIP Journal on Advances in Signal Processing* (2010). http://asp.eurasipjournals.com/content/2010/1/319065

34. Xie, Y., Guo, B., Li, J. and Stoica, P. "Novel multistatic adaptive microwave imaging methods for early breast cancer detection", *EURASIP Journal on Applied Signal Processing*, 2006(20), pp. 1-13 (2006).

35. Naghibi, T., Namvar, M. and Behnia, F. "Optimal and robust waveform design for MIMO radars in the presence of clutter", *Signal Processing*, **90**(4), pp. 1103-1117 (2010).

36. Feng, D., Li, X., Lv, H., Liu, H. and Bao, Z. "Two-sided minimum-variance distortionless response beamformer for MIMO radar", *Signal Processing*, **89**(3), pp. 328-332 (2009).

37. Chen, J., Gu, H. and Su, W. "A new method for joint DOD and DOA estimation in bistatic MIMO radar", *Signal Processing*, **90**(2), pp. 714-718 (2010).

38. Jin, M., Liao, G. and Li, J. "Joint DOD and DOA estimation for bistatic MIMO radar", *Signal Processing*, **89**(2), pp. 244-251 (2009).

39. Aittomaki, T. and Koivunen, V. "Performance of MIMO radar with angular diversity under swerling scattering models", *IEEE Journal of Selected Topics in Signal Processing*, **4**(1), pp. 101-114 (2010).

40. Berger, C.R., Demissie, B., Heckenbach, J., Willett, P. and Zhou, S. "Signal processing for passive radar using OFDM waveforms", *IEEE Journal of Selected Topics in Signal Processing*, **4**(1), pp. 226-238 (2010).

41. Radmard, M., Khalaj, B., Chitgarha, M., Nazari Majd, M. and Nayebi, M. "Receivers' positioning in multiple-input multiple-output digital video broadcast-terrestrial-based passive coherent location", *IET Radar, Sonar & Navigation*, **6**, pp. 603-610 (2012).

42. Radmard, M., Karbasi, S., Khalaj, B. and Nayebi, M. "Data association in multi-input single-output passive coherent location schemes", *IET Radar, Sonar & Navigation*, **6**(3), pp. 149-156 (2012).

43. Raout, J., Santori, A. and Moreau, E. "Passive bistatic noise radar using DVB-T signals", *IET Radar, Sonar & Navigation*, **4**(3), pp. 403-411 (2010).

Biographies

Mojtaba Radmard received BS, MS and PhD degrees in Electrical Engineering from Sharif University of Technology, Tehran, Iran, where he is currently working as a postdoctoral degree researcher. His research interests include MIMO systems, passive coherent location, signal processing and speech processing.

Mohammad Nazari-Majd received BS and MS degrees (high honors) in the field of communications from Sharif University of Technology, Tehran, Iran, where he is currently working towards his PhD degree. His research interests include MIMO radars, noise radars, detection theory and radar signal processing. Mr. Nazari-Majd was also a member of the Iranian Physics' Olympiad team in 2008.

Mohammad Mahdi Chitgarha received BS and MS degrees in the field of communications from Sharif University of Technology, Tehran, Iran where he is now a PhD degree candidate. He was ranked 1st in both MS and PhD degree national university entrance exams. His research interests include MIMO radars, radar signal processing, detection theory, and speech signal processing.

Babak Hosein Khalaj received his BS degree from Sharif University of Technology, Tehran, Iran, in 1989, and MS and PhD degrees from Stanford University, Stanford, CA, in 1993 and 1996, respectively, all in Electrical Engineering. He joined KLA-Tencor in 1995 as a Senior Algorithm Designer working on advanced processing techniques for signal estimation

and from 1996 to 1999, he was with Advanced Fiber Communications and Ikanos Communications. Since then, he has been a Senior Consultant in the area of Data Communications, and a visiting professor at CEIT, San Sebastian, from 2006 till 2007. Prof. Khalaj has also been senior member of the Advanced Communications Research Institute (ACRI) at Sharif University of Technology, where he has been faculty member since 1999. His main research interests include wireless networking, smart antenna technologies, sensor networks and digital signal processing.

Mohammad Mahdi Nayebi received BS and MS degrees from Sharif University of Technology, Tehran, Iran, and PhD degree in Electrical Engineering, from Tarbiat Modarres University, Tehran, Iran.

He joined Sharif University of Technology faculty in 1994. His main research interests are radar signal processing and detection theory.